2021 43rd Annual International Conference of the
IEEE Engineering in Medicine & Biology Society (EMBC)
Oct 31 - Nov 4, 2021. Virtual Conference

Effects of Scaffold Electrical Properties on Electric Field Delivery in Bioreactors.

João Meneses, Sofia R. Fernandes, Nuno Alves, Paula Pascoal-Faria* and Pedro Cavaleiro Miranda*

Abstract— **In tissue engineering, cell culture scaffolds have been widely used in combination with electrical stimulation to promote multiple cellular outcomes, like differentiation and proliferation. Nevertheless, the influence of scaffolds on the electric field delivered inside a bioreactor is often ignored and requires a deeper study. By performing numerical analysis in a capacitively coupled setup, this work aimed to predict the effects of the scaffold presence on the electric field, considering multiple combinations of scaffold and culture medium electrical properties. We concluded that the effect of the scaffold on the electric field in the surrounding culture medium was determined by the difference in electrical conductivity of these two materials. The numerical simulations pointed to significant variations in local electric field patterns, which could lead to different cellular outcomes and confound the interpretation of the experimental results.**

I. INTRODUCTION

In recent years, a plethora of cellular biological effects are attributed to the external application of electric fields (EFs), magnetic fields (MFs) and electromagnetic fields (EMFs) [1]. EFs can regulate a variety of cell functions, including cellular growth, adhesion, reorganization of the cytoskeleton, contractility, differentiation and proliferation, by modulating the activation of intracellular pathways involved in the secretion of relevant proteins and increased gene expression. The effects of EFs have been demonstrated in different cell types and at different development phases, but the mechanisms behind cell-EF interactions are not completely understood, strongly limiting the applications of EFs [2]. In Tissue Engineering, multiple electrical conductive and non-conductive biomaterials have been developed for tissue culture substrates in a variety of forms (porous scaffolds, films, nanofibers, coatings) [3]. After cell seeding, the culture is subjected to an electrical stimulation employing capacitive-coupled (CCoupled) or direct-coupled (DCoupled) setups, to achieve the desired cell function regulation.

This research was funded by the Fundação para a Ciência e a Tecnologia (FCT) and Centro2020 through the following Projects: CDRSP UIDP/04044/2020 and and UIDB/04044/2020, PAMI—ROTEIRO/0328/2013 (No 022158); FCT Project Stimuli2BioScaffold ref. PTDC/EMESIS/32554/2017; Bone2Move ref. PTDC/CVT-CVT/31146/2017; MATIS - Ref. CENTRO-01-0145-FEDER-000014-3362; Instituto de Biofísica e Engenharia Biomédica (IBEB) is supported by Fundação para a Ciência e Tecnologia (FCT), Portugal, under Grant UIDB/00645/2020. Also supported by UID/BIO/04565/2020.

J. M. and N. A. and P. P-F. are with the Centre for Rapid and Sustainable Product Development (CDRSP-IPLeiria), 2430-028 Marinha Grande, Portugal. Corresponding authors (P.P-F and P.C.M.): paula.faria@ipleiria.pt and pcmiranda@fc.ul.pt

S. R. F. and P. C. M. are with IBEB, Faculdade de Ciências, Universidade de Lisboa, 1749-016 Lisboa, Portugal.

* joint last authors.

Despite the ubiquitous presence of cell support material in experimental electrical stimulation protocols, its impact on delivered EFs has mostly been neglected. An understanding of this impact when selecting the scaffold geometry and material is the main motivation behind the present study. In this study, a widely utilised CCoupled setup based on Brighton's original work [4], [5], is used to analyse this impact. A geometrical model for this setup was created, and a sensitivity analysis was performed through the finite-element method (FEM). After validating our model against the experimental measures made by Brighton *et al.* [4], [5], we introduced an orthogonal scaffold in the culture medium and ran an extensive sensitivity analysis of the delivered EF as a function of the electrical parameters of the scaffold material and culture medium (electrical conductivity and permittivity).

II. MATERIALS & METHODS

A. 3D Model Geometry Construction

1) Brighton FEM Model - Cell Culture Chamber Without Scaffold: The 3D model replicating Brighton's experimental setup, as described in [4], [5], was constructed with SOLIDWORKS software (version 2018, Dassault Systemes SolidWorks Corporation, France). The geometry is composed by 5 co-axial cylindrical domains with a diameter of 33 mm (Fig. 1A): two stainless steel electrodes, with a thickness of 1 mm; two glass coverslips placed between the electrodes and the culture medium, with a thickness of 0.16 mm; one cell culture medium chamber that occupies the entire central region, with a thickness of 10 mm. The dimensions that haven't been specified in Brighton's descriptions of the setup, were estimated based on the drawing present in [5], and on similar commercially available parts.

2) Brighton FEM Model - Cell Culture Chamber With Scaffold: To the previously described 3D model, an orthogonal scaffold was added at the bottom of the cell culture medium chamber (Fig. 1B). This scaffold is composed of alternating horizontal layers of 300 $\mu\mathrm{m}$ filaments, whose centers are 600 $\mu\mathrm{m}$ apart. Consecutive layers are rotated by 90º. In order to avoid meshing and numerical problems associated with point contacts and sharp edges, the tips of each filament were rounded, and an overlap of 20 $\mu\mathrm{m}$ was introduced between adjacent horizontal layers, which are separated by 580 $\mu\mathrm{m}$. For the same reason, the bottom of the scaffold is placed 350 $\mu\mathrm{m}$ above the bottom of the chamber. Three equidistant and equal-sized rectangular prism regions-of-interest were added to the 3D model to allow detailed studies in these regions (Fig. 1C, 1D).

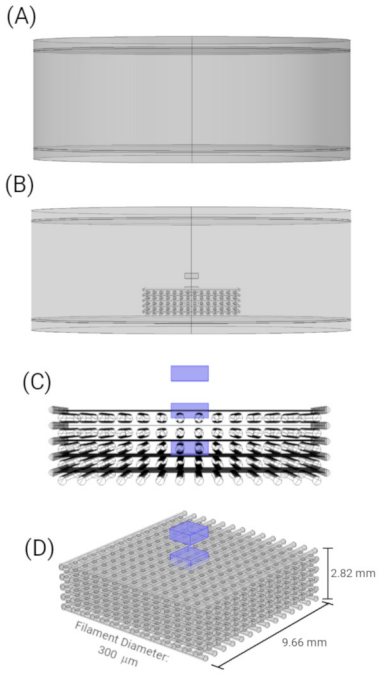

Fig. 1. Model geometry. (A) 3D model of Brighton's experimental setup, composed of 5 distinct domains: two electrodes (top and bottom); two glass coverslips (top and bottom); one culture medium domain (central). (B) 3D model with orthogonal scaffold placed at the bottom of the cell culture medium chamber. (C) Three equidistant and equal-sized rectangular prism regions-of-interest (tinted blue), representing the external, interface and internal regions of the scaffold environment. (D) Volumetric view of the orthogonal scaffold with overall dimensions and the regions-of-interest (tinted blue).

B. Finite Element Analysis (FEA)

Finite element analysis was conducted with the AC/DC module of COMSOL Multiphysics (version 5.2a, www.comsol.com, Stockholm, Sweden). The Electric Current (ec) physics interface was selected, considering a frequency-domain study at 60 kHz. A 3D physics-controlled mesh was also generated in COMSOL for each model (with and without scaffold), with the finer mesh option. Both models are composed of three common materials: stainless steel for electrodes (σ: 4.032×10^6 $\mathrm{S\,m^{-1}}$, ϵ_r: 1); cover glass N1 insulating walls (σ: 1.0×10^{-13} $\mathrm{S\,m^{-1}}$, ϵ_r: 6.85); and cell culture medium. The model with scaffold also contains the scaffold material, the properties of which were varied in a parametric sweep study together with the culture medium properties (Table I). Following Brighton's work [4], [5], an electric potential boundary condition of 44.81 V was added to the top surface of the top electrode, and a ground boundary condition was added to the bottom surface of the bottom electrode. COMSOL BiCGStab stationary iterative solver was used to run this parametric sweep study.

C. Sensitivity and Spatial Distribution Analysis

Sensitivity analysis was performed by means of a one-at-a-time variation method, applied to the results obtained from the COMSOL parametric sweep study. This parametric sweep study generated 540 different solutions, one for each combination of the input parameters described in Table I, with electrical conductivities and permitivities values obtained from [6], [7], [8].

Electric field data were then exported from COMSOL Multiphysics software to text file format, for further post-processing in custom made python scripts, using Pandas, Matplotlib and SALib libraries. These python scripts were used to generate the plots and histograms for sensitivity and spatial distribution analysis. Sensitivity analysis was also performed by the method of Delta Moment-Independent Measure, implemented in python SALib library accordingly with the original works of [9], [10]. Sensitivity and spatial distribution analysis were independently performed for each region-of-interest (external, interface and internal), where only the culture medium nodes data were considered. Spatial distribution analysis was performed on three real scaffold materials from the tissue engineering field (Thermoplastic [11], Hidrogel [12], Metalic [13]), and also on a control scaffold with the same material electrical properties of the cell culture medium (no effect of scaffold presence is expected under this condition).

TABLE I
SENSITIVITY ANALYSIS STUDY PARAMETERS.

Culture Medium Electrical Conductivity σ_{cm} ($\mathrm{S\,m^{-1}}$)	**Culture Medium** Relative Permittivity ϵ_{cm} (dimensionless)
1.1, 1.5, 1.9	50, 80.1, 90
Scaffold Electrical Conductivity σ_s ($\mathrm{S\,m^{-1}}$)	**Scaffold** Relative Permittivity ϵ_s (dimensionless)
1.0×10^{-14}, 0.001, 0.005, 0.01, 0.05, 0.1, 0.5, 1.1, 1.3, 1.5, 1.7, 1.9, 10, 50, 100, 150, 300, 500, 1000, 7.5×10^5	1, 2.2, 80.1

III. RESULTS

A. Validation of Brighton 3D FEM Model

Brighton *et al.* [4], [5] reported that with their experimental setup and using a 60 kHz sinusoidal wave of 44.81 V amplitude, they were able to generated an electric field of 20 $\mathrm{mV\,cm^{-1}}$ (2.0 $\mathrm{V\,m^{-1}}$) and a current density of 300 $\mathrm{\mu A\,cm^{-2}}$ (3.0 $\mathrm{A\,m^{-2}}$). Our 3D FEM model without scaffold predicts an average electric field of 2.1 $\mathrm{V\,m^{-1}}$ and an average current density of 3.2 $\mathrm{A\,m^{-2}}$ in the culture medium. Thus, by comparison, we can conclude that this 3D FEM model accurately predicts the values obtained experimentally in Brighton *et al.* [4], [5].

B. Sensitivity Analysis

This analysis was performed on the results obtained for Brighton's setup including the scaffold. Sensitivity analysis results from the Delta Moment-Independent Measure are shown in Table II. The higher the First Order significance, the greater the contribution of the corresponding parameter to the variation of the electric field magnitude. As expected, in

the external ROI it is the conductivity of the culture medium that has the greatest impact on the electric field. Conversely, in the internal ROI it is the conductivity of the scaffold that has the greatest impact, followed by the conductivity of the culture medium.

TABLE II
DELTA MOMENT-INDEPENDENT MEASURE RESULTS.

EXTERNAL ROI

Parameter	Delta	Conf.	1st Order Significance	Conf.
σ_{cm}	0.58	0.02	0.64	0.04
ϵ_{cm}	0.28	0.01	0.17	0.01
σ_s	0.09	0.01	0.09	0.05
ϵ_s	0.28	0.01	0.17	0.01

INTERFACE ROI

Parameter	Delta	Conf.	1st Order Significance	Conf.
σ_{cm}	0.51	0.02	0.63	0.06
ϵ_{cm}	0.20	0.01	0.09	0.01
σ_s	0.40	0.03	0.68	0.03
ϵ_s	0.20	0.01	0.09	0.01

INTERNAL ROI

Parameter	Delta	Conf.	1st Order Significance	Conf.
σ_{cm}	0.39	0.02	0.45	0.04
ϵ_{cm}	0.13	0.01	0.04	0.01
σ_s	0.53	0.03	0.84	0.03
ϵ_s	0.13	0.01	0.04	0.01

Sensitivity analysis on FEM solutions from the parametric sweep study were plotted and grouped by colour code in Fig. 2, with different colours representing different electrical conductivities of the culture medium. Each row shows plots of the average, maximum and minimum electric field magnitude in one of the three regions-of-interest as a function of the electrical conductivity of the scaffold. Variations in the relative permittivities of the culture medium and scaffold had no noticeable impact on the electric field. Hence, a single point in these graphs represents the value of the electric field for all values of the permitivitties.

We can observe that at 60 kHz the parameters that most influence magnitude of the eletric field in a bioreactor are the electrical conductivities of both the culture medium and the scaffold material. All plots in Fig. 2 analysis may be split into three regions: one region corresponding to insulating materials with electrical conductivity lower than 1.0×10^{-2} $\mathrm{S\,m^{-1}}$, where changes in scaffold electrical conductivity generate small variations in the electric field, for a fixed cell culture medium conductivity; another region corresponding to conductive materials with electrical conductivity greater than 1.0×10^{2} $\mathrm{S\,m^{-1}}$, where changes in scaffold electrical conductivity generate small variations in the electric field; and a transition region, where an almost linear relation between scaffold electrical conductivity and the electric field magnitude can be observed in the average plots (left column of Fig.2). On the other hand, in the maximum and minimum plots, local minima and maxima arise when the electrical conductivity of the scaffold matches that of the cell culture medium.

C. Spatial Distribution Analysis

Spatial distributions of the electric field magnitude are presented in Fig. 3. As expected, the control scaffold, which has the same electrical properties of the cell culture medium, introduces no changes in electrical field, which remains uniform (Fig. 3 - A1, B1, C1, H1). When the scaffold is more insulating or more conductive than the cell culture medium, the electric field distribution is greatly affected. A more insulating scaffold material generates local hot zones and cold zones inside the scaffold (Fig. 3 - A2, B2, C2, H2, A3, B3, C3, H3). A more conductive scaffold material shields the surrounding culture medium from the external electric field stimulation (Fig. 3 - A4, B4, C4, H4). The histograms in the bottom row show that the presence of insulating scaffolds spreads the range of the delivered electrical field magnitude, while the presence of conductive scaffolds reduces this range.

IV. DISCUSSION

Our FEA results were obtained for a 60 kHz sinusoidal wave of 44.81 V amplitude and show that the scaffold effect in electric stimulation (ES) delivery cannot be ignored. However, different waveforms, with different frequency spectra, will produce changes in the delivered electrical field. It is expected that waveforms with frequencies below 60 kHz, will generate lower electric field magnitudes for the same voltage, but maintain the EF spatial patterns shown in Fig. 3. The effects introduced by the relationship between scaffold conductivity and culture medium conductivity will predictably remain valid for frequencies lower than the studied 60 kHz. However, for far higher frequencies, it is expected that the influence of both permittivities on the electric field surrounding the scaffold becomes more significant.

Sensitivity analysis data obtained from one-at-a-time variation method (Fig. 2) and by delta moment-independent measures (Table II), reveals that permittivities of the scaffold and culture medium have a residual effect on the delivered EF. In contrast, the electrical conductivities of the scaffold and culture medium regulate the major effects presented in this work. More insulating scaffolds generate a surrounding electric field pattern with peaks and troughs, amplifying and attenuating the delivered EF. This effect is attributed to the opposition produced by the scaffold to the electric current flow. The EF pattern is geometry dependent, hence scaffolds with different configurations from the orthogonal one studied in this work will present different spatial patterns of EF. In turn, more conductive scaffolds, will shield the surrounding culture medium from the external applied electric field, delivering a strongly attenuated EF, more independent of the scaffold geometry.

According to the literature [12], [14], many scaffold materials have electrical conductivities that fall in the transition region identified in Fig. 2. This factor, together with the experimental variability of the conductivity of culture media, raises *per se* the impossibility of comparison between electrical stimulation works that did not take into account the effect introduced by the scaffold presence in those experimental

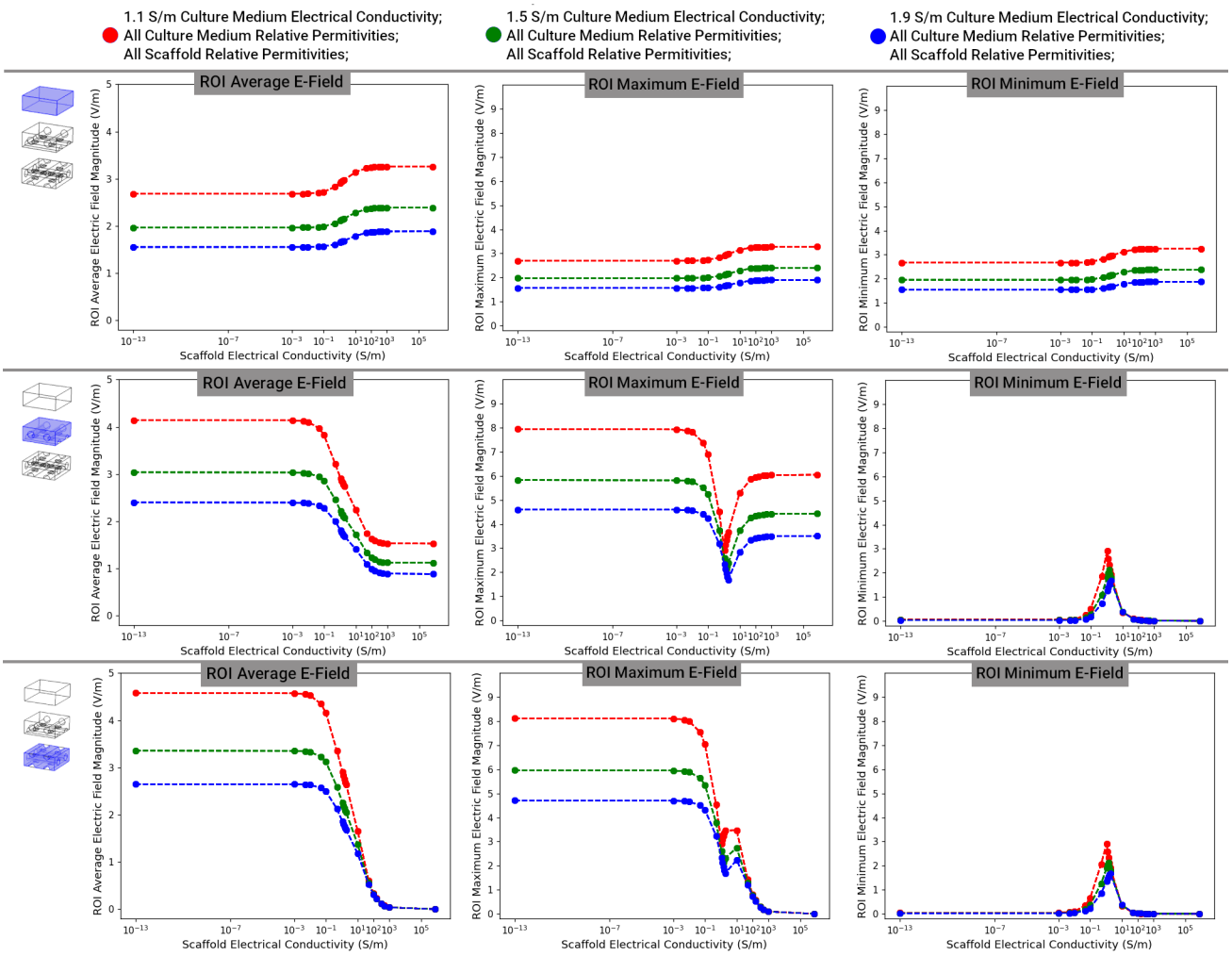

Fig. 2. One-at-a-time sensitivity analysis of the electric field magnitude per region-of-interest. Each row contains plots for the average, maximum and minimum electrical field versus the scaffold material electrical conductivity. Each plot contains all the 540 different solutions (each solution is represented by one point), and data are colour code by culture medium electrical conductivity. The plotted data under analysis only contains solutions from the culture medium nodes.

conditions. This comparison would be decisive to standardize a specific stimulation protocol with the use of scaffolds for a specific cellular outcome.

A recent work [15] focused on tailoring the electrical conductivity of a hydrogel material used as cell culture substract for maximizing the effect on cell transmembrane potential (TMP), also utilizing Brighton's setup and protocol. Their findings are in line with our results, by concluding that hydrogel conductivity plays an important role in the external electrical stimulation effect. The authors observed that lower conductivity hidrogel contributes to increase TMP values and that the effect of the hydrogel permittivity on ES is negligible. Also, our current work, does not address directly the effect on TMP, but it does show that lower conductivity materials generate higher EFs peaks and troughs in their surroundings, probably contributing also to higher TMP values. Our conclusions apply to different classes of materials and includes a broader range of electrical conductivities and permittivities. The predicted effects of the scaffold's presence on the induced EF reported here must be taken into account when designing and conducting electrical stimulation experimental protocols, as they may strongly influence the outcomes and the understanding regarding the electrical stimulation effectiveness.

V. CONCLUSIONS

Our work shows that the insertion of a cellular scaffold in an electrical stimulation setup influences the surrounding electrical field. According to our predictions, the presence of a scaffold can deeply influence the electric field spatial patterns in its local environment, by introducing local peaks and troughs or by completely shielding the effects of external stimulation. The predicted EF strongly depends on the electrical properties of the scaffold. Follow up research should carefully choose scaffold materials to increase the effectiveness of EF delivery aiming at a specific cellular outcome. We also recommend that conclusions from previous works be revised taking into consideration this neglected effect.

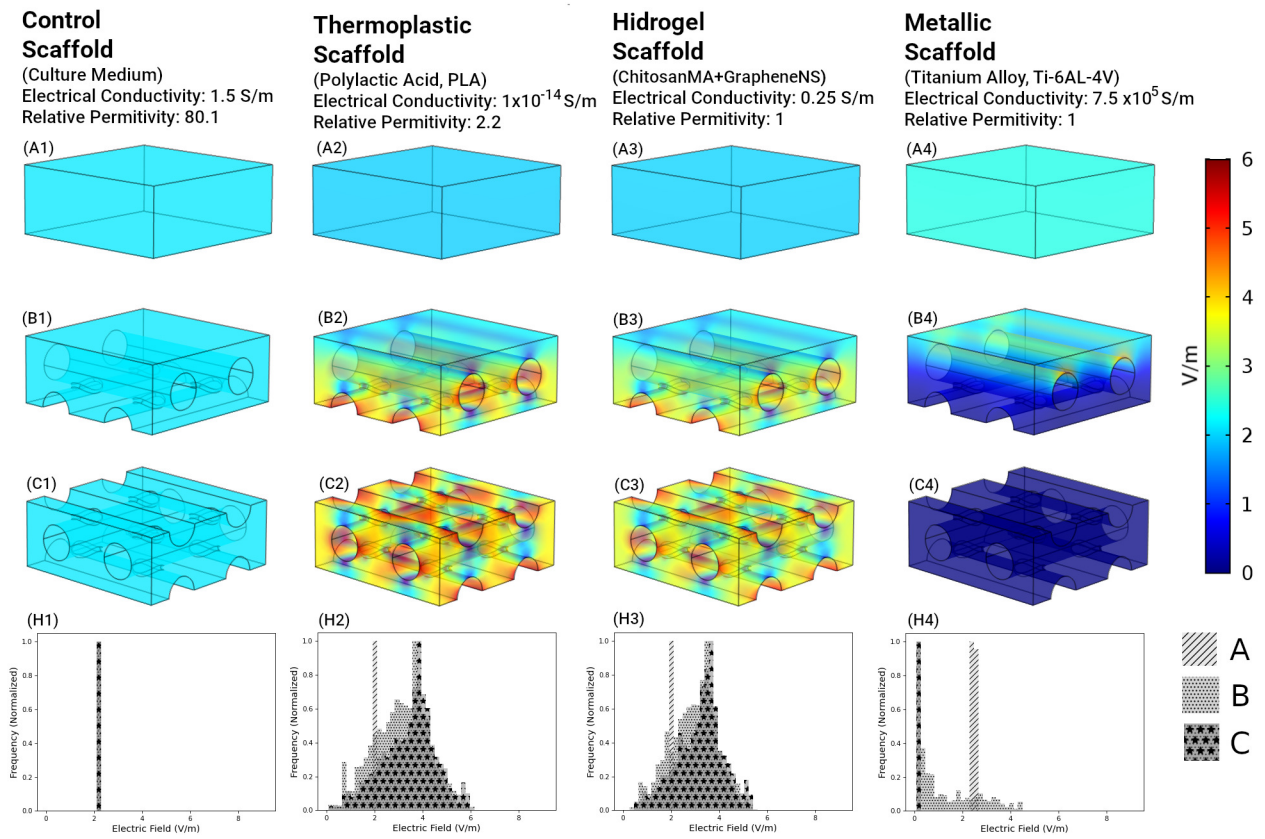

Fig. 3. Spatial distribution of the electric field under fixed culture medium electrical parameters (σ: 1.5 $\mathrm{S\,m^{-1}}$, ϵ_r: 80.1) and fixed external electric stimulation (Brighton's conditions). Each column of the figure presents the predicted result for the specified scaffold material at the regions-of-interest labeled from A to C. In the bottom row, a normalized frequency histogram of the electric field magnitude is presented.

REFERENCES

[1] R. H. Funk, T. Monsees, and N. Özkucur, "Electromagnetic effects – from cell biology to medicine," *Progress in Histochemistry and Cytochemistry*, vol. 43, no. 4, pp. 177 – 264, 2009. [Online]. Available: http://www.sciencedirect.com/science/article/pii/S0079633608000375

[2] T. Taghian, D. A. Narmoneva, and A. B. Kogan, "Modulation of cell function by electric field: a high-resolution analysis," *Journal of The Royal Society Interface*, vol. 12, no. 107, p. 20150153, 2015. [Online]. Available: https://royalsocietypublishing.org/doi/abs/10.1098/rsif.2015.0153

[3] R. Dong, P. X. Ma, and B. Guo, "Conductive biomaterials for muscle tissue engineering," *Biomaterials*, vol. 229, p. 119584, 2020. [Online]. Available: http://www.sciencedirect.com/science/article/pii/S0142961219306830

[4] C. T. Brighton and W. P. McCluskey, "Response of cultured bone cells to a capacitively coupled electric field: Inhibition of camp response to parathyroid hormone," *Journal of Orthopaedic Research*, vol. 6, no. 4, pp. 567–571, 1988. [Online]. Available: https://onlinelibrary.wiley.com/doi/abs/10.1002/jor.1100060414

[5] C. T. Brighton, E. Okereke, S. R. Pollack, and C. C. Clark, "In vitro bone-cell response to a capacitively coupled electrical field. The role of field strength, pulse pattern, and duty cycle," *Clin Orthop Relat Res*, no. 285, pp. 255–262, Dec 1992.

[6] N. Gavish and K. Promislow, "Dependence of the dielectric constant of electrolyte solutions on ionic concentration: A microfield approach," *Phys. Rev. E*, vol. 94, p. 012611, Jul 2016. [Online]. Available: https://link.aps.org/doi/10.1103/PhysRevE.94.012611

[7] E. L. Bennett, C. Song, Y. Huang, and J. Xiao, "Measured relative complex permittivities for multiple series of ionic liquids," *Journal of Molecular Liquids*, vol. 294, p. 111571, 2019. [Online]. Available: http://www.sciencedirect.com/science/article/pii/S0167732219327187

[8] A. P. Mazzoleni, B. F. Sisken, and R. L. Kahler, "Conductivity values of tissue culture medium from 20°c to 40°c," *Bioelectromagnetics*, vol. 7, no. 1, pp. 95–99, 1986. [Online]. Available: https://onlinelibrary.wiley.com/doi/abs/10.1002/bem.2250070111

[9] E. Borgonovo, "A new uncertainty importance measure," *Reliability Engineering and System Safety*, vol. 92, no. 6, pp. 771 – 784, 2007. [Online]. Available: http://www.sciencedirect.com/science/article/pii/S0951832006000883

[10] E. Plischke, E. Borgonovo, and C. L. Smith, "Global sensitivity measures from given data," *European Journal of Operational Research*, vol. 226, no. 3, pp. 536 – 550, 2013. [Online]. Available: http://www.sciencedirect.com/science/article/pii/S0377221712008995

[11] V. J. Hegde, O. Gallot-Lavallée, and L. Heux, "Overview on thermal and electrical properties of biodegradable polymers," in *2015 IEEE 11th International Conference on the Properties and Applications of Dielectric Materials (ICPADM)*, 2015, pp. 540–543.

[12] T. Distler and A. R. Boccaccini, "3d printing of electrically conductive hydrogels for tissue engineering and biosensors – a review," *Acta Biomaterialia*, vol. 101, pp. 1 – 13, 2020. [Online]. Available: http://www.sciencedirect.com/science/article/pii/S1742706119306099

[13] NDE. (2021) Conductivity and resistivity values for titanium and alloys. [Online]. Available: https://www.nde-ed.org

[14] R. Balint, N. J. Cassidy, and S. H. Cartmell, "Conductive polymers: Towards a smart biomaterial for tissue engineering," *Acta Biomaterialia*, vol. 10, no. 6, pp. 2341 – 2353, 2014. [Online]. Available: http://www.sciencedirect.com/science/article/pii/S1742706114000671

[15] J. Zimmermann, T. Distler, A. R. Boccaccini, and U. van Rienen, "Numerical simulations as means for tailoring electrically conductive hydrogels towards cartilage tissue engineering by electrical stimulation," *Molecules*, vol. 25, no. 20, 2020. [Online]. Available: https://www.mdpi.com/1420-3049/25/20/4750